International Journal of Research in Engineering and Science (IJRES)
ISSN (Online): 2320-9364, ISSN (Print): 2320-9356
www.ijres.org Volume 11 Issue 5 ǁ May 2023 ǁ PP. 547-561

Thermal-hydraulic analysis of the modified topaz irradiation process at ETRR-2

H.F. Elbakhshawangy[1], O. S. Abd El-Kawi[1] and Abdelfatah Abdelmaksoud[1]
[1]*Reactors department, Nuclear Research Center, Egyptian Atomic Energy Authority, Egypt*

ABSTRACT
In this paper, three dimensional CFD thermal-hydraulic analysis is carried out for the modified irradiation process of topaz in ETRR-2 (Egyptian Second Research Reactor). Topaz is modeled as porous media using ANSYS FLUENT computer code. Study of the effect of parameters such as Reynolds number (Re) and porosity (ε) on the flow and heat transfer characteristics is performed for both the cases of the modified irradiation process in which there are Boron-Carbide plates at the sides of the topaz irradiation box and the previous irradiation process without the plates. The study is performed for Reynolds number (Re) in the range $2.32x10^3 \leq Re \leq 9.36x10^3$ *and porosity (ε) in the range* $0.3 \leq \varepsilon \leq 0.5$*. Determination of the location and value of the maximum temperature for all the cases are presented with determination of the conditions under which onset of nucleate boiling occurs. Average values of temperature and heat transfer coefficient for topaz and the Boron Carbide plates are presented at different values of Re and ε with a comparison between the case of irradiation with Boron-Carbide plates and the case of irradiation without them. Two correlations relating Nu with Re and ε one for topaz and the other for the plates are presented in the studied range of Re and ε. The ideal value of porosity from the thermal-hydraulic point of view is determined.*

Keywords: *ETRR-2, porosity, Reynolds number, thermal-hydraulic, topaz irradiation*

Date of Submission: 09-05-2023 Date of acceptance: 20-05-2023

I. INTRODUCTION

Gemstones are pieces of mineral crystals which, upon cutting and polishing, are used to make jewelry. Some gemstones colors can be changed upon irradiation [1,2,3]. The irradiation process can be accomplished in nuclear reactors by neutrons [4], by electron irradiation from electron beams in an accelerator [5], or by gamma rays from Cobalt 60 irradiators [6]. The most commonly type of these gemstones whose colors can be changed upon irradiation is topaz. Topaz is an aluminum fluorosilicate with a fairly constant chemical composition $Al_2SiO_4(OH,F)_2$ [7]. The most common type of topaz is colorless and of little worth. The most common type of colored topaz which is used in jewelry is blue topaz. Electron irradiation from high energy accelerators is used for mass production of large quantities of blue topaz [8]. The advantage of gamma rays irradiation is the high activity which causes the irradiation process of topaz to be done in short time. Neutron irradiation of topaz has the advantage of producing darker blue stones than the cases of irradiation by electrons or gamma due to the ability of neutrons to penetrate the crystal causing more change in the crystal structure. Topaz irradiation by neutrons is carried out in nuclear reactor and this process results in high energy deposition in the stones. If the temperature of topaz stones approaches 300 ^oc damage and de-coloration of topaz stones will occur. In addition, if the temperature is too high, flaking can occur during post-irradiation handling. A typical temperature during irradiation should be between 100^oc and 150^oc, so topaz stones must be cooled during irradiation [9]. ETRR-2 is used for topaz irradiation. Irradiation process was performed in an Aluminum irradiation box without thermal neutron shield. During the irradiation process, radio-isotopes were produced resulting in deposition of radioactivity. Therefore after irradiation, topaz stones had to be stored for a period of time to reduce the radioactivity to the limits for radioactive material transfer, and this period is called the release time. The release time of topaz was calculated based on a certain radioactivity limit which depended on local national regulations. Long period of time ranging from one to three years depending on the impurities in topaz was needed to reach the release limit. The thermal neutron part in the neutron flux had the main contribution for the production of the isotopes resulting in the high radioactivity in topaz. Whereas, the fast neutron part is the one needed for topaz irradiation. So a modification was suggested by neutron- calculation people to suppress the thermal neutrons inside the irradiation box. This modification depends on the shielding of the Aluminum irradiation box from each side by a plate of Boron-Carbide as Boron is a thermal neutron absorber. In the irradiation process, topaz contained in the irradiation box is placed in the irradiation grid surrounding the reactor core and cooled through the pool cooling system by forced downward flow of water inside the box. Flow of water through topaz stones is considered as flow through porous media. Heat transfer to a fluid passing through a channel filled with porous

materials was studied by several researchers. Many correlations exist in the literature for the estimation of the heat transfer coefficient in porous media, i.e between the porous material and the flowing fluid. Among those are: The Ranz–Marshall correlation [10]: $Nu = 2+0.6\ Re^{0.5}Pr^{0.33}$, valid in the range $0 \leq Re \leq 200$, Whitaker correlation [11]: $Nu =(2+0.4Re^{1/2}+0.06Re^{2/3})Pr^{0.4}(\mu/\ \mu_s)^{1/4}$ valid in the range: $0.71 \leq Pr \leq 380$, $3.5 \leq Re \leq 7.6\times10^4$, $1.0 \leq (\mu/\mu_s)$. Macias – Mechin et al. correlation [12]: $Nu = 1.27+2.66(Re/\varepsilon)^{0.56}Pr^{-0.41}((1-\varepsilon)/\ \varepsilon)^{0.29}$. One of the most reliable correlations for calculating heat transfer coefficient between the solid particles and the fluid is the correlation by Gnielinski [13] :

$Nu = f(\varepsilon)\ Nu_s$, $f(\varepsilon) = 1+1.5(1-\varepsilon)$, $Nu_s=2+ (Nu_t^2+Nu_L^2)^{0.5}$, $Nu_L= 0.664Pr^{1/3}(Re/\ \varepsilon)^{1/2}$,

$Nu_t = [0.037(Re/\ \varepsilon)^{0.8}Pr]/[1+2.433(Re/\ \varepsilon)^{-0.1}(Pr^{2/3}-1)]$.

With respect to the heat transfer from the Boron carbide plate, many correlations in the literature were developed for the purpose of the estimation of the heat transfer from a heated plate immersed in porous media. Among these correlations are: Cheng correlation [14]: $Nu = 0.854\ Pe^{0.5}$. Spechia et al. [15] considered the wall heat transfer coefficient to be the sum of a flow-dependent and a flow-independent heat transfer coefficient. So, they proposed the correlation: $Nu = Nu_{fin}+Nu_{fd}$ .They predicted the flow-independent contribution to the wall heat transfer coefficient by applying the correlation of Kunii and Smith [16]: $Nu_{fin} = 2\varepsilon + (1-\varepsilon)/(K_f/K_s+\Phi)$. They suggested that stagnant heat conduction occurs in parallel through a fraction ε, of the surface of the wall that is not covered by particles and through a fraction (1- ε) that is covered. Φ is the characteristic distance between the wall and the surface of the particles and depends on the aspect ratio N of the bed with the following correlation between Φ and N: $\Phi = 0.0024N^{1.58}$. For the convective contribution (flow dependent part), only empirical correlations were used: $Nu_{fd} = 0.083Re^{0.91}$ which is valid in the range: $10 \leq Re \leq 1200$, $Nu_{fd} = 1.23Re^{0.53}$, valid in the range: $1200 \leq Re \leq 1000$. Y. Demirel et al [17] studied experimentally the wall-fluid heat transfer coefficient and radial conductivity in a packed bed. They determined two values for Nu; one related to the bulk fluid temperature and the other related to the extrapolated fluid temperature at the wall. El-Morshedy [18] studied the thermal-hydraulic characteristics of topaz irradiation at ETRR-2 before the modification of adding Boron-Carbide plates to the irradiation box. He developed a mathematical model to evaluate the cooling process through a part of the irradiation grid at the ETRR-2 containing one irradiation topaz box. The coolant flow rate and temperature distribution along the model channels including topaz irradiated box are predicted. The temperature distribution in one irradiated topaz stone was estimated also. The purpose of this work is to perform a case study of the thermal-hydraulic characteristics of the modified process of topaz irradiation at ETRR-2 after the addition of Boron-Carbide plates inside the irradiation box at its four sides. A comparison with the corresponding characteristics before the modification (i.e without the Boron-Carbide plates) is also presented. For this purpose, one topaz box is numerically simulated using Ansys-Fluent commercial computer code. The irradiation is performed in the irradiation grid surrounding the reactor core. The components in the irradiation grid such as beryllium reflectors and the irradiated materials are cooled by a 150 m^3/h of water flowing in the downward direction.

Nomenclature

A	Surface area
C	Inertial loss coefficient
D	Equivalent hydraulic diameter, m
d_p	Particle diameter, m
F_{fo}	Darcy friction factor for single-phase liquid
g	Acceleration gravity, m/s^2
G	Mass flux, kg/m^2s
h	Heat transfer coefficient, $W/m^{2o}c$
k	Thermal conductivity, $W/\ m^oc$
L	Active length, m
N	Aspect ratio of the porous media bed
Nu	Nusselt number (hD/K)
P	Pressure, N/m^2
Pa	particle
Pe	Pecklet number = u_bD/α
Pr	Prandtl number
q	Generated heat,W
Re	Reynolds number ($u_bD\rho/\mu$)
T	Temperature, ^oc
u_b	Coolant velocity through topaz box, m/s
V_l	Liquid specific volume, m^3/kg
V_{li}	Liquid specific volume at entrance, m^3/kg

V coolant velocity, m/s

Greek letters

α Permeability
ε Porosity
ρ Density, kg/m^3
μ Fluid viscosity, NS/m^2
σ Surface roughness, m
Φ Characteristic distance between the wall and surface of the particle

Subscripts

av Average
C Centre
Bc Boron carbide
eq Equivalent
f Refers to conditions at bulk fluid
fd Flow dependent
fin Flow independent
i Refers to conditions at inlet
L Laminar
O Refers to conditions at outlet
S Refers to conditions at solid surface
To Topaz
t Turbulent
w Refers to conditions at the wall
wa Water

II. NUMERICAL MODELING

2.1 Geometry and boundary conditions

A Thermal-hydraulic numerical simulation of the modified irradiation process of one topaz irradiation box in ETRR-2 is presented. The irradiation box is made from Aluminium with 6.6 cm x 6.6 cm cross section, and a length of 82 cm as shown in Fig.1 (a). Fig.1 (b) shows the numerical mesh. Whereas Fig.1 (c) shows a closed view of the inlet region of the coolant, where a length of 8 cm of the irradiation box is left empty, i.e does not have topaz. The 0.2 cm dimension in this view represents the thickness of the Boron Carbide plates. The Boron Carbide plates are placed at each side in the box. Each plate is fabricated from 24% Boron, 6% Carbon, and 70% Aluminium. The Boron Carbide is at the centre of the plate and surrounded from all sides by Aluminium. The plate is 82 cm length, 6.4 cm width, and 0.2 cm thickness. The boundary conditions of the simulation domain and the main data required for the simulation are shown in table.1.

Table.1 Boundary conditions and main data required for the simulation

Parameter	Value
Topaz density	3.573 g/cm^3
Topaz thermal conductivity	11.28 W/mk
Topaz specific heat	83.6 J/m^{o}c
Box internal dimensions with B.C. plates	6.2x6.2x82 cm
Box hydraulic diameter	6.2 cm
Physical domain boundary conditions	• Velocity at box inlet in the downward direction • Pressure at box outlet which has the value of pressure at outlet from irradiation grid • Wall (No slip conditions) at all walls • Two zones are defined: 1. Box inlet region where porous model is not activated 2. Topaz region where porous media model is activated.
Box downward inlet velocities	1.4, 2.5, 5, 7, and 9 cm/s
Topaz porosity	30, 35, 40, 45, and 50 %
Heat generation in topaz (Case with Boron carbide plates)	$(1-\epsilon)$ * 0.17 w/cm^3 [7]
Heat generation in Boron carbide plates	3 w/cm^3 [7]

Heat generation in topaz (Case without Boron carbide plates)	$(1-\epsilon)$ * 8 w/cm^3 [18]

2.2 Mathematical modeling and numerical solution

The aim of this modeling is to make a case study of the comprehensive thermal hydraulic characteristics for the modified process of topaz irradiation in ETRR-2.For this purpose, 3D CFD simulation is carried out using commercial CFD software ANSYS FLUENT 20 R2. Evaluation of the thermal and flow fields for the process of topaz cooling is performed. During irradiation, topaz is cooled by flow of water in the downward direction through the topaz irradiation box. The numerical solution is carried out under the following assumptions:

1- The flow is assumed at steady state, incompressible and turbulent.
2- Thermo physical properties of water coolant, topaz, and Boron carbide are assumed constant.
3- Thermal radiation is neglected.

The 3D equations describing the present study are:

$$\frac{\partial}{\partial x_i}(\rho V_i) = 0.0 \qquad (1)$$

$$\frac{\partial}{\partial x_j}(\rho V_i V_j) = -\frac{\partial P}{\partial x_i} + \frac{\partial \tau_{ij}}{\partial \tau_j} + \rho g_{x_i} \qquad (2)$$

$$\frac{\partial}{\partial x_i}[V_i(\rho E + P] = -\frac{\partial}{\partial x_i}\left(K\frac{\partial T}{\partial x_i}\right) \qquad (3)$$

where, i: indicates 1, 2, and 3 and τ_{ij} is the viscous shear stress. The variables V; ρ; P; T; E and K are the water flow velocity, density, pressure, temperature, energy and thermal conductivity respectively. The standard k- ε model is used for modeling of turbulence as it gives accurate results for such problems of internal flow. The heat transfer coefficient in topaz or over the Born-Carbide plate surface is calculated from the following equations:

For topaz: $h_{To} = q_{To}/A_{To}(T_{avTo}-T_i)$ (4)

For Boron-Carbide plate: $h_{Bc} = q_{Bc}/A_{Bc}(T_{avBc}-T_i)$ (5)

In the previous equations h, q, A, T are the heat transfer coefficient, the heat generated, surface area, and temperature respectively. The equivalent density ρ_{eq}, conductivity k_{eq}, and viscosity μ_{eq} can be calculated from the equations of the homogeneous mixture model:

$\rho_{eq} = \epsilon \rho_{wa} + (1-\epsilon)\rho_{To}$ (6)

$k_{eq} = \epsilon k_{wa} + (1-\epsilon) k_{To}$ (7)

$\mu_{eq} = \epsilon\mu_{wa} + (1-\epsilon)\mu_{To}$ (8)

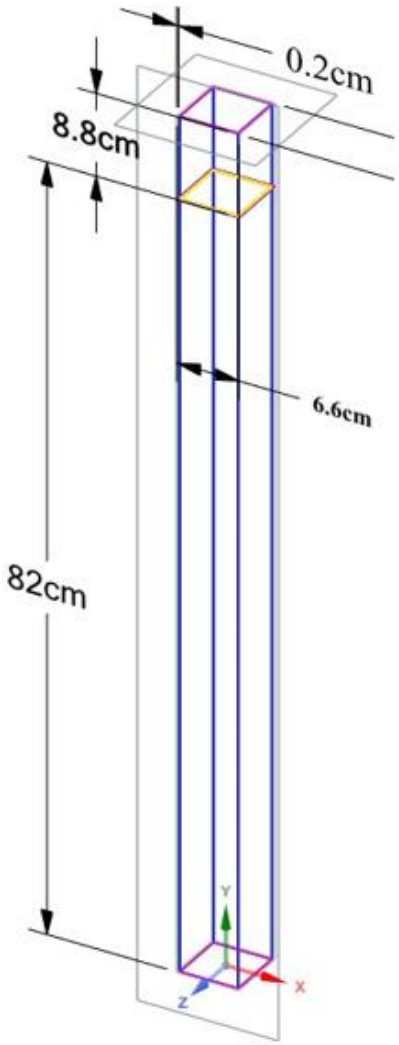

a) Studied geometry

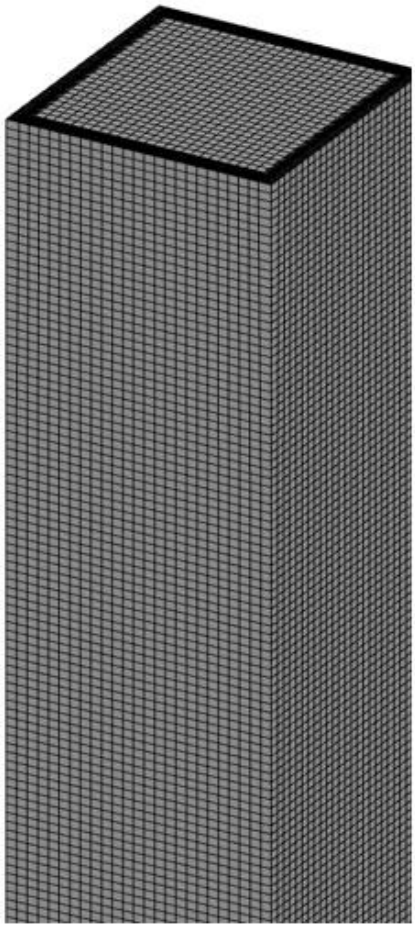

b) Numerical mesh

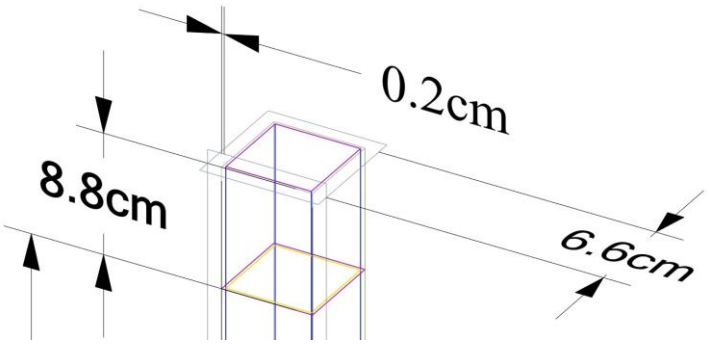

c) Close view of the inlet region

Fig.1 The simulation domain

2.3 Modeling of the porous media

2.3.1 Governing equations

Flow through porous media is modeled by a modified Navier-Stokes equation in which a source term associated with the resistance caused by the porous media is added to the standard Navier-Stokes equation [19]. The loss term is composed of two parts. A part accounts for viscous loss and another part responsible for inertia loss. This source term is represented mathematically in the form:

$$S_i = -\left(\sum_{j=1}^{3} D_{ij}\mu V_{i_j} + \sum_{j=1}^{3} C_{ij}\frac{1}{2}\rho|V|V_j\right) \quad (9)$$

Where S_i is the source term in the direction x, y, or z, $|V|$ is the magnitude of the velocity and D and C are the

Darcy and Inertial matrices respectively. In case of considering a homogeneous porous medium, D will be a diagonal matrix of coefficient 1/∝, and C will be also a diagonal matrix, so the source term will be in the form: $S_j = -\left(\frac{\mu}{\propto} V_j + \frac{1}{2} C\rho|V|V_j\right)$ (10)

Where α is the permeability, C is the inertial loss coefficient.

2.3.2 Determination of the porous media model input parameters

The momentum sink due to the porous medium, represented by Eq.10, contributes to the pressure gradient in the porous zone, creating a pressure drop that is proportional to the fluid velocity (or the squared velocity) in the cell. The permeability and inertial loss coefficient in the topaz filled zone (porous zone) of the irradiation box is calculated using Ergun correlation for estimation of pressure gradient in porous media which is a semi-empirical correlation applicable over a wide range of Reynolds numbers and for many types of packing. Ergun correlation:

$$\frac{|\Delta P|}{L} = \frac{150\mu}{d_p^2}\frac{(1-\varepsilon)^2}{\varepsilon^3}V + \frac{1.75\rho}{d_p}\frac{(1-\varepsilon)}{\varepsilon^3}V^2 \qquad (11)$$

By comparing equations 10, and 11

$\frac{1}{\alpha} = \frac{150}{d_p^2}\frac{(1-\varepsilon)^2}{\varepsilon^3}$ and $C = \frac{3.5}{d_p}\frac{(1-\varepsilon)}{\varepsilon^3}$

2.3.3 Grid independent test

Figure 2 shows the variation of maximum temperature in the topaz box with the number of computational cells for the case of porosity of 30% and Re of 9.36E3. From this figure, it can be shown that for a number of cells greater than about 290000, the maximum temperature remains constant at about 335.94 K. Increasing the number of cells than the previous value will not affect the results but is considered time consuming without any benefit. So, this number of cells is used for the rest of the analysis.

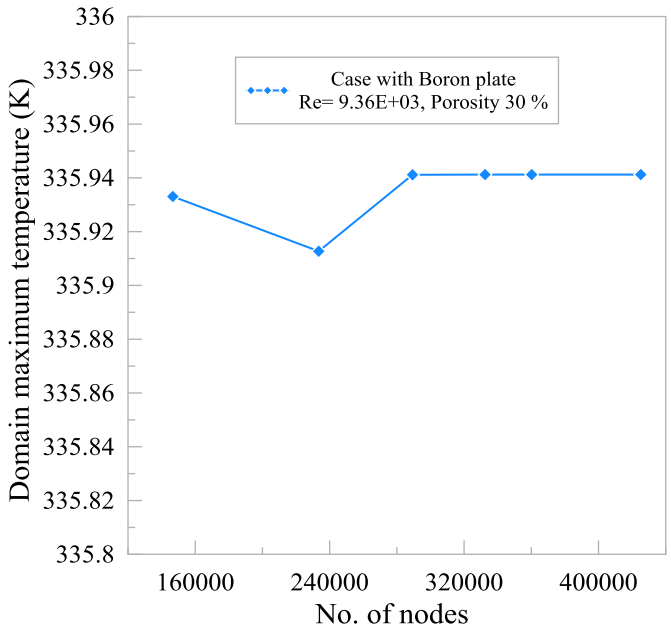

Fig.2 Variation of maximum topaz temperature with number of grid cells

III. MODEL VALIDATION

Fig. 3 shows the variation of the average Nu over the Boron-Carbide plate with average Re for the flow through the topaz box at different porosity. The empirical correlation derived by Y. Demirel et al [17] for heat transfer from a heated plate embedded in porous media is represented on this figure for the purpose of comparison with the present results and model validation. As in this correlation the particle diameter d_p is used as the characteristic length in Re and Nu, d_p is used as the characteristic length in average Re and Nu of the results shown in Fig.3. The correlation of Y. Demirel et al is $Nu = 0.047Re^{0:927}$. This correlation is applicable in the range $4.5 < D/d_p < 7.5$, $200 < Re < 1450$. As seen from this figure, Y. Demirel et al. correlation gives a good prediction of the present results especially at low and moderate values of Re. The comparison reveals a

maximum error of 22.5% at the maximum value of Re = 1450 in this figure. The reason for this trend returns to the fact that for the correlation of Y. Demirel et al., the bulk fluid temperature is used for the calculation of Nu whereas in the present study, as topaz and water are modeled as homogeneous porous media, inlet fluid temperature is used for the calculation of Nu. Therefore, for the case of Demirel et al. correlation, increasing Re causes the average plate temperature as well as the bulk fluid temperature to decrease such that Nu increases linearly with Re. For the case of the present study the average plate temperature decreases with Re, whereas the inlet temperature remains constant. So, as shown in Fig.3 for the curves of the present study, as Re increases Nu increases with Re linearly but in different slopes. As the decrease in the plate temperature with Re is more pronounced at low and moderate values of Re, Nu increases in lower slopes as Re increases as shown in Fig.3. So, as Re increases, Nu of the present results increases in a slope lower than the corresponding one of Demirel et al correlation resulting in more divergence between the two results. The curves of the present study show that increasing the porosity causes Nu to decrease at the same Re as increasing the porosity causes the heat transfer coefficient h to decrease as will be discussed in section 4.2 (see Fig.10.c). This will be accompanied by decrease in the equivalent thermal conductivity k_{eff} of topaz-water porous medium as increasing the porosity means greater water fraction in the porous medium. As the thermal conductivity of water is less than the corresponding one of topaz, the equivalent conductivity of the porous medium decreases with the porosity. So, increasing the porosity causes h as well as k_{eff} to decrease but the effect of h is higher than the corresponding effect of k_{eff} so the resultant will be a decrease in Nu with the porosity ($Nu = h\, k_{eff}/D$).

IV. RESULTS AND DISCUSSION

4.1 Effect of Re and ε on thermal and flow fields

4.1.1 Temperature contours

The effect of Re on the temperature contours is shown in figures 4 and 5 for the modified case of topaz irradiation with Boron-Carbide plates for a porosity value of 30%. Figures 4 and 5 show 3D temperature contours through the whole topaz box and 2D temperature contours at the outlet of the flow from the box, at different values of Re, respectively. Figure 4 shows that minimum temperature through the box is at the top where there are neither plates nor particles (the empty inlet region of 8.8 cm at the top of

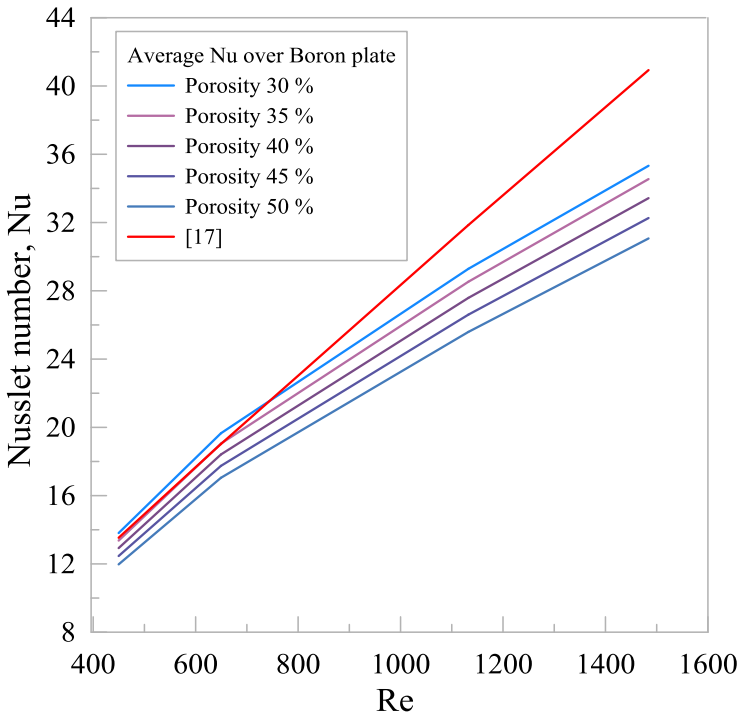

Fig.3 Comparison between Nu of the present study with that of the correlation of Y. Demirel et al. [17]

the box in Fig.1). As the box walls are adiabatic, the temperature at the whole inlet zone remains roughly constant at fluid inlet temperature value. As the fluid passes in the downward direction through the box, it gets in contact with both the plates and the particles removing the heat generated within them and the temperature increases gradually towards the downward direction. At any cross section along the length of the box, a uniform minimum temperature zone exists in the middle of the box and the temperature increases towards the plates as

shown in figures 4 and 5 because the heat generated in the plates is much greater than that generated in topaz particles. Hence, at any cross section along the topaz box length, the maximum temperature is at the box corner due to the double heating effects at the wall corners as shown in Fig 4 and 5. The value of the maximum temperature increases towards the outlet from the box as shown in Fig.4. Therefore, the maximum temperature is located in the corner of the box at the outlet of the coolant. Continue moving in the downward direction after the inlet region, the regions of high temperature expand from the sides towards the middle at expense of the regions with low temperature. The lowest temperature remains in the middle at any section, but this region narrows upon moving towards the downward direction as shown in Fig.4. By increasing Re, the uniform low temperature region in the middle of the box expands at expense of the higher temperature ones in both the longitudinal and transverse directions and the maximum temperature value (at the box corner) decreases as shown in figures 4 and 5 respectively.

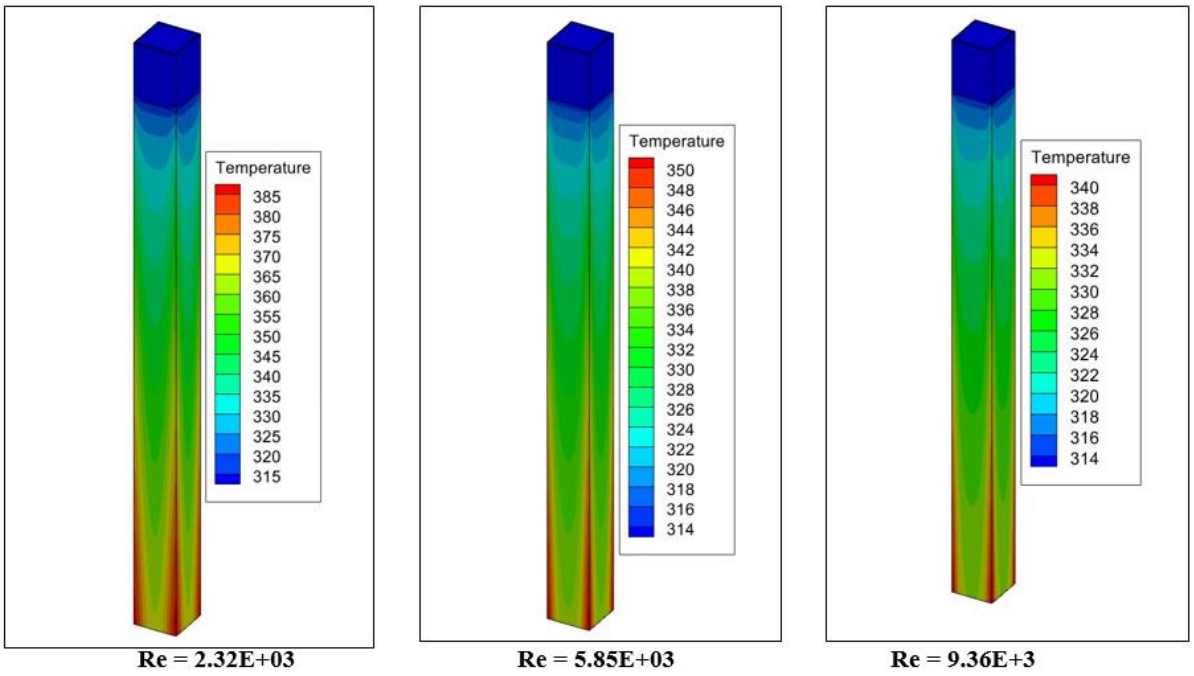

Fig.4 Temperature contours for topaz box with Boron-Carbide plates

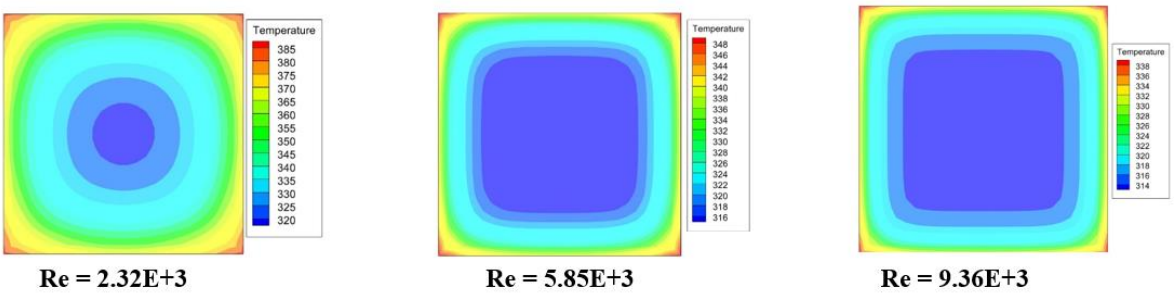

Fig.5 Temperature contours at outlet from topaz box with Boron-Carbide plates

4.1.2 Local temperature profiles

Figures 6.a and 6.b show the variation of local temperature profiles at the middle of topaz box with porosity for both the cases of irradiation with and without Boron-Carbide plates respectively. Figure 6.c shows the corresponding temperature profile at the centreline of the Boron-Carbide plate surface. The results are obtained at constant value of Re = $2.23x10^2$. As shown from Fig.6.a, in the upper part of the box near the entrance (Y=0.9 m), the temperature profiles rise very slightly from what it was at the entrance, which is 313 K, and the profiles are identical for all values of the porosity. This is because in the case of the presence of the plates, the heat generated in topaz is very little (see table 1), and the differences in the heat generated as a result of the difference in porosity are almost negligible. In addition, the temperature in the middle of the box is not affected yet, in the zone immediately after the entrance, by the heat generated in the plates. This causes the curves to congruent with each other. As the coolant flows through the box in the downward direction, the temperature increases due to the continuous removal of heat from the plates and topaz. As a result, the

temperature in the middle of the box begins to be noticeably rise as compared with the entrance region as it is affected by the heat generated in the plates which is much higher than the heat generated in topaz. This rise in temperature is higher for the lower porosity. This is because lower porosity means higher equivalent density of topaz-water mixture (see Eq.6) and hence lower flow velocity as the continuity equation must be satisfied. The shape of the curves changes from the linear shape by approaching the exit from the box. This occurs as a result of being affected by the accumulation of both the heat generated in topaz and that transferred from the plates, which is much greater than that generated in topaz. As shown from figure 6.b the situation for the case without the plates is different. In this case, there is no heat generated except for that generated in topaz, but it is much greater than that generated in the previous case, since the plates act as a thermal neutron absorber thus reducing the heat generated in topaz. Therefore, in the case without plates, the curves representing the different porosity values are distinguished from each other from the beginning of the box immediately after the entrance, and they are all straight lines due to homogeneous heat generation in topaz, so the curves are similar to the case of flow with internal heat generation in the fluid. The lower the porosity is the greater the slope of the curve and this is due to the increase in the generated heat with the lower porosity in addition to the lower velocity of the fluid due to the increase in the equivalent density as discussed above. Comparison of figures 6.a and 6.b show that the values of temperature in the case of irradiation without the plates are higher than the case of existence of the plates for all the values of porosity. This is because the generated heat to be removed by the coolant is much greater without the plates. As shown from Fig.6.c, the temperature values along the length of the plate at the middle of its surface decrease with decreasing the porosity. The reason for this trend returns to the increase in the equivalent conductivity in the radial direction with decreasing the porosity which causes improvement in the heat transfer from the plates to topaz stones adjacent to the plates. At the top edge of the plate, the temperature increases abruptly from the value corresponding to the inlet fluid temperature to the temperature of the upper part of the heated plate. This is the reason for the large slope of the curve immediately after the inlet region. After this region, the temperature increases gradually at a lower slope. Figure 7 shows the effect of Re on temperature profiles at different porosity along the box corner line for the modified case of irradiation with Boron-Carbide plates. At the box corner, highest temperature exists at any cross section along the topaz box because of the double heating effect as discussed earlier in the previous section. Figure 7 shows that the trend of the temperature profiles resembles this of Fig.6.c and the reason for this trend is the same as discussed in Fig.6.c. In section 4.1.1, it was shown that the maximum temperature at any cross section along the length of the topaz box is at the box corner. Fig.7 shows that the maximum temperature is at the exit from the box for all of the cases and its value increases with the porosity and decreases with Re. As shown from Fig.7.a, onset of nucleate boiling can occur at the lower part of the box corner for porosity greater than 0.4 and a value of Re = 2.23×10^2. As at these conditions, the temperature is greater than 393 K which is the estimated temperature for onset of nucleate boiling at the local operating pressure. So bubbles are expected to appear during irradiation at these conditions. Increasing flow rate and hence Re above the previous value, can prevent the onset of nucleate boiling as shown in Fig.7 b,c .

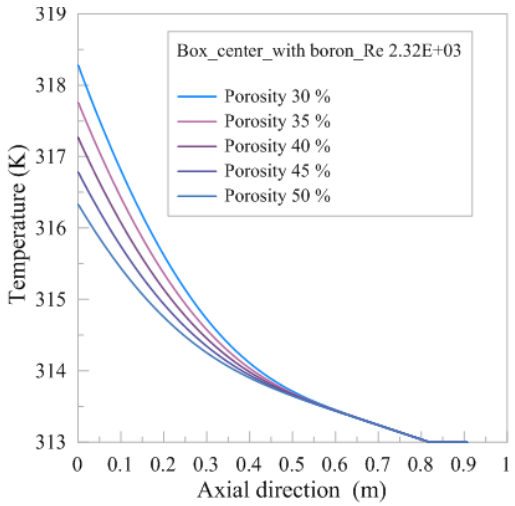

a) Box center line with Boron-Carbide

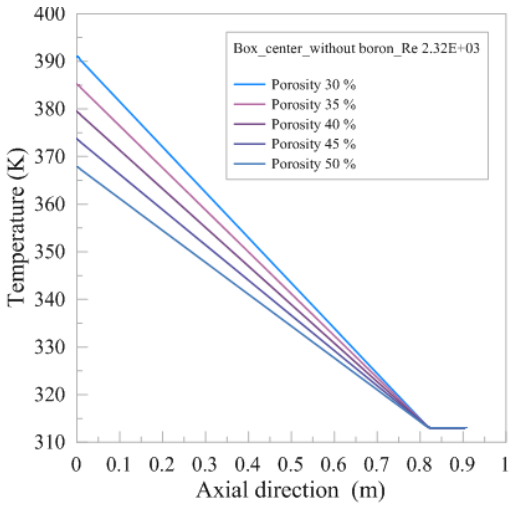

b) Box center line without Boron- Carbide

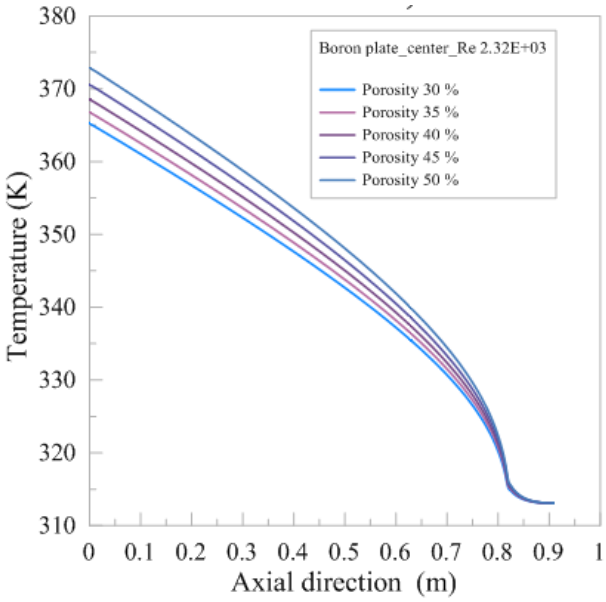

C) Center line of Boron-carbide plate surface

Fig.6 Variation of local temperature profiles with porosity at constant Re

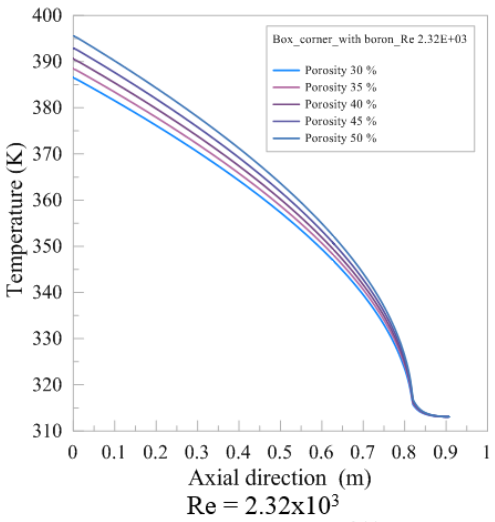

$Re = 2.32x10^3$

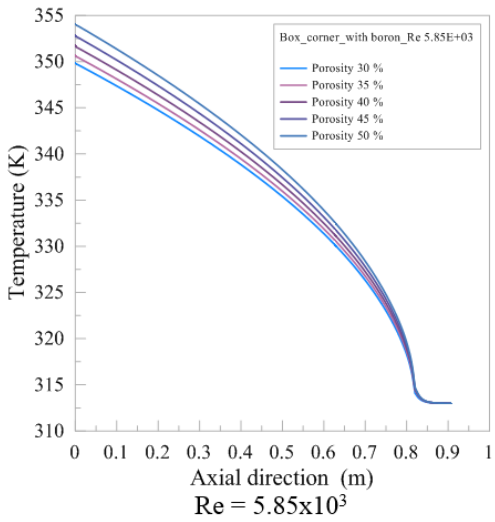

$Re = 5.85x10^3$

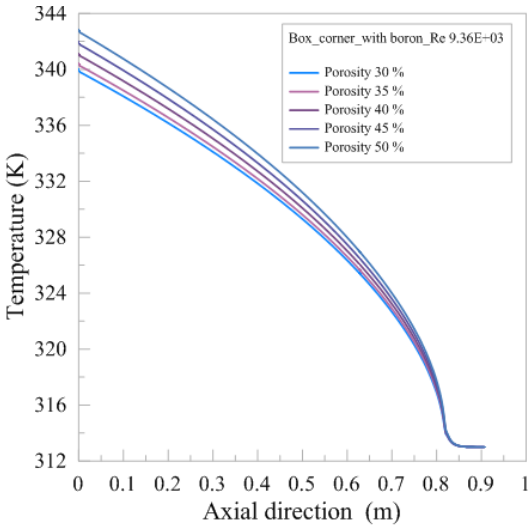

$Re = 9.36x10^3$

Fig.7 Variation of local temperature profiles at the box corner with porosity at different values of Re

4.1.3 Local flow profiles

Figures 8.a and 8.b show the variation of the local velocity and pressure profiles, in the middle of the topaz box, with porosity at constant value of Re= 2.32E3 respectively. From Fig.8.a it can be shown that at the inlet of the box (at a height of 0.908 m in Fig.8.a) the velocity value is the one corresponding to the uniform inlet velocity of the boundary condition which is of a value of 1.4 cm/s at Re= 2.32E3. As the coolant flows from the inlet, its velocity increases rapidly because of the rapid formation of the boundary layer and its increasing thickness until reaching a maximum value approximately in the middle of the inlet empty region (about 5 cm from the inlet). By approaching the region filled by porous medium, the velocity starts to decrease from its maximum value until reaching the porous medium where it has a value that remains constant throughout the porous medium until the exit from the irradiation box. The effect of porosity is to cause this constant value of velocity to increase with the porosity value as shown in Fig.8.a. The reason for this returns to treating the porous medium as a homogeneous mixture of water and topaz which has an equivalent density greater that that exists at the inlet where there is only pure water (see Eq.6). Hence, as the continuity equation must be satisfied, the velocity in the porous zone is less than that at the inlet zone that does not contain topaz. In the porous zone, increasing the porosity causes the equivalent density to decrease resulting in higher flow velocity which remains constant till the exit from the box as shown in Fig.8.a. Figure 8.b shows that the local static pressure value at the middle of the topaz box decreases linearly by passing through the porous zone until reaching a fixed value at the outlet. This is the value corresponding to the pressure at the outlet from the irradiation grid and which is set as a boundary condition at the outlet. As low porosity value hinders the flow, the pressure drop through the porous zone increases by decreasing the porosity as shown in Fig.8.b.

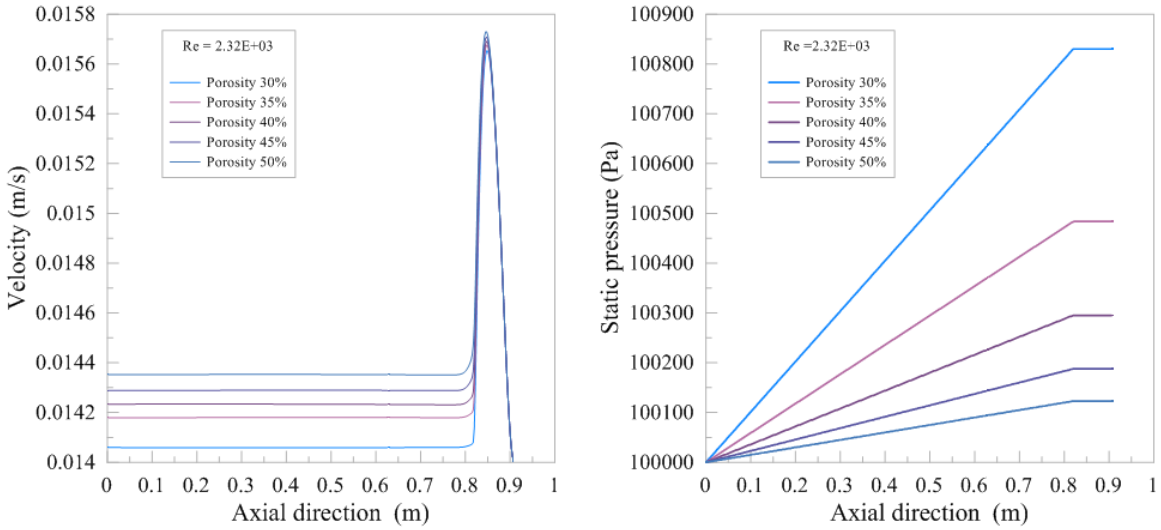

a)Velocity profiles b) pressure profiles

Fig.8 Variation of local flow profiles in the middle of the box with porosity at constant value of Re

4.2 Effect of Re and ε on heat transfer characteristics

Figures 9.a and 9.b show the variation of average topaz temperature with average Re at different values of porosity for both the cases of irradiation without and with Boron-Carbide plates respectively. Fig.9.c shows the variation of average plate temperature with average Re at different values of porosity. From these figures, it can be shown that the temperatures for the case of irradiation without the Boron- carbide plates are greater than the corresponding ones for irradiation with the plates. The reason for this is the fact that the plates act as a thermal neutron shield resulting in reduction in the heat generation in the topaz. So, the generated heat in the topaz in case of irradiation without the plates is much greater than the sum of heat generated in the topaz and the Boron-Carbide plates together in the case of irradiation with the plates (see the values for heat generation in table 1). This results in a rise in the temperature values of topaz in the absence of the plates. The temperature difference between the two cases is higher at lower Re. The average temperature decreases with Re for all the cases and the reason is obviously due to the better cooling as higher Re means higher coolant velocity. The average temperature increases with the decrease in the porosity in the case of irradiation without the plates. This can be attributed to the fact that by reducing the porosity, the heat generation increases (see table.1) and the coolant velocity decreases owing to the increase in the equivalent density in the porous region as the continuity equation must be accomplished.

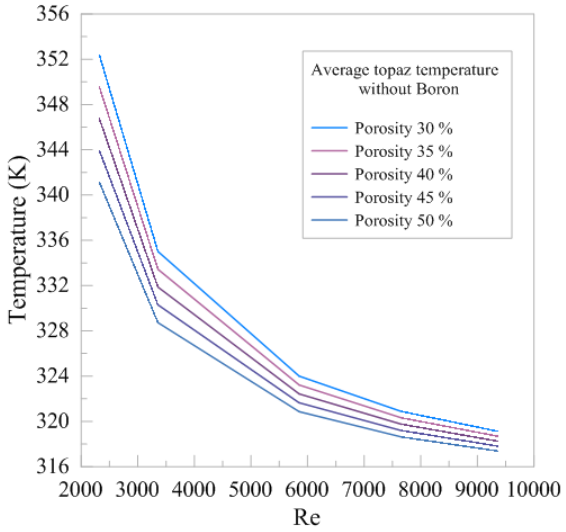

a) Topaz temperature without the plates

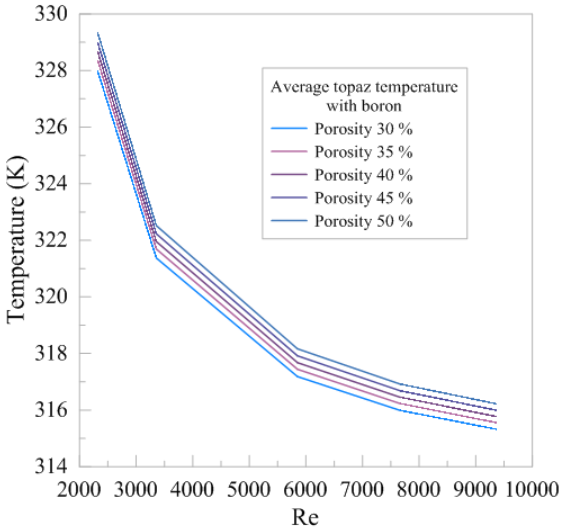

b) Topaz temperature with the plates

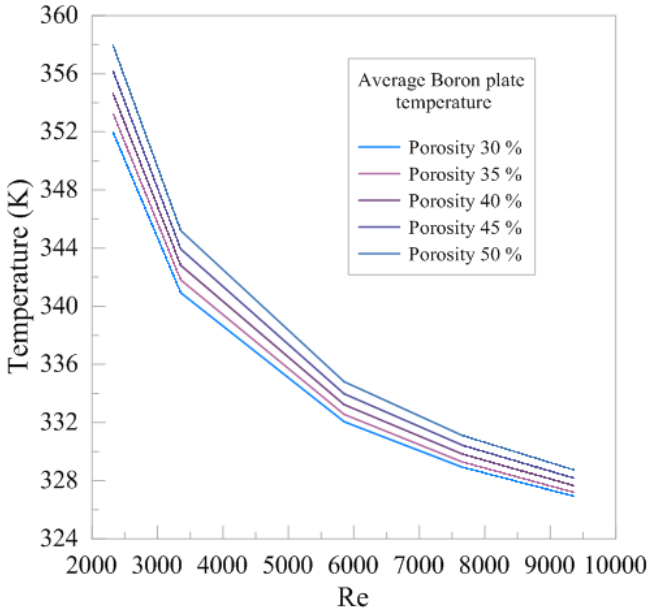

C) Plate temperature

Fig.9 Variation of average temperature with average Re at different values of ε

On the contrary, the average topaz temperature for the case of irradiation with the Boron- Carbide-plates. In this case, both the average topaz and plate temperature decrease by decreasing the porosity (Fig.9.b and 9.c respectively). In these two cases, this opposite trend of temperature can be explained from Fig.10. Figure 10 shows the variation of the average heat transfer coefficient h with Re at different values of porosity for topaz without and with the Boron Carbide plates and for the plates (Fig.10.a, 10.b, 10.c respectively). From Fig.10.c, it can be shown that the heat transfer coefficient on the plate surface increases with decreasing the porosity and this can be attributed to the increase in the equivalent thermal conductivity in the radial direction (see Eq.7). Thus higher plate heat transfer coefficient results in lower temperature at the plate surface. Consequently, with less porosity, the parallel layer adjacent to the plate becomes of lower temperatures, unlike the case for the middle of topaz (see the results of Fig.6.a) in which the middle temperature increases with less porosity. The effect of the temperatures of topaz layers adjacent to the plates on the average temperature of topaz is greater than the effect of the temperature in the middle, so that the result is a decrease in the average temperature of topaz with less porosity. The heat transfer coefficient drawn in Fig.10 is calculated from equations 4,5 – section 2.2 for topaz and Boron-Carbide plates respectively. For the case of topaz, decreasing the porosity causes both the generated heat and the total surface area of topaz to increase in the same proportion, and the factor affecting the value of the heat transfer coefficient is (T_{avTo}-T_i). By decreasing the porosity, (T_{avTo}-T_i) increases for the case of irradiation without the Boron –Carbide plates and decreases for the case of

irradiation with them as deduced from figures 9.a and 9.b respectively. So, by decreasing the porosity, the heat transfer coefficient decreases for the case of irradiation without the plates and increases for irradiation with them as shown in Fig.10.a, and 10.b respectively. The values of topaz heat transfer coefficient in the case without the plates are much

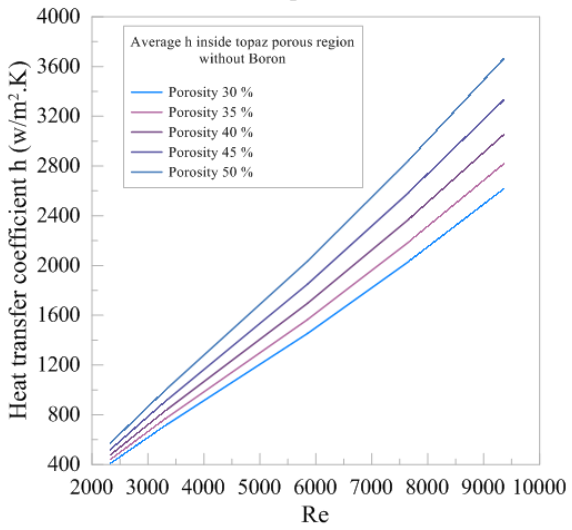

a) h for topaz without the plates

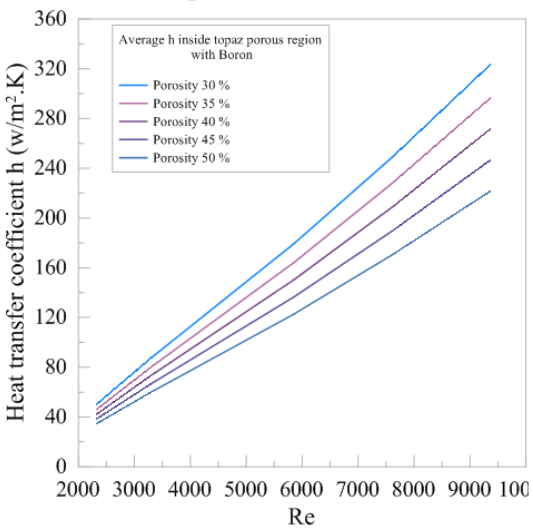

b) h for topaz with the plates

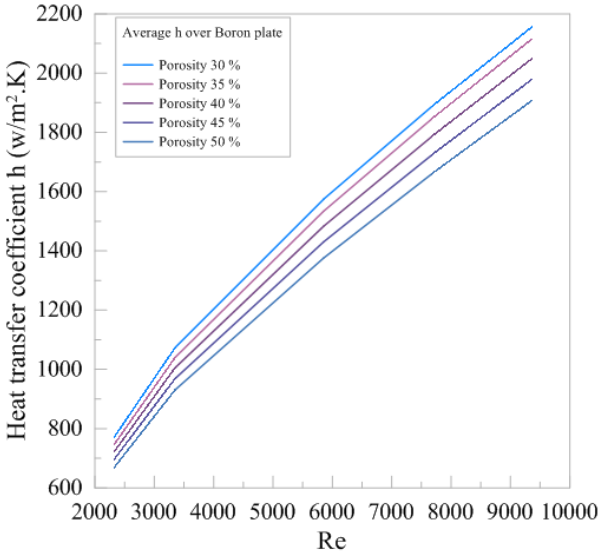

c) h for the plates

Fig.10 Variation of average h with average Re at different values of ε

higher than those for the case with the plates due to the much higher heat generation in topaz for the case of irradiation without the plates as discussed above. Figure 10.c shows that, the heat transfer coefficient increases by reducing the porosity. The reason for this trend is the decrease in the value of (T_{avbc}-T_i) (see Eq.5 in section 2.2), as both the generated heat and surface area of the plates are constant and do not depend on the porosity. The heat transfer coefficient increases with Re for all of the cases as shown in Fig.10 due to cooling improvement.

4.3 Determination of the ideal porosity value

Figure 11 shows the variation of the average topaz temperature with porosity at a fixed value of Re = 7.67×10^3, and at a constant heat generation (i.e does not depends on porosity as discussed earlier) for the case of irradiation with the plates. From this figure it can be shown that the average temperature decreases with porosity until a certain value of porosity at which a minimum value of temperature is obtained. After this value, further

increase of the porosity causes the average temperature to increase. The reason for this trend is that by increasing the porosity, two effects on the average temperature of topaz occur. The first is that with increasing the porosity, the equivalent density of topaz-water mixture decreases as deduced from Eq.6, and the result of this is an increase in the velocity of water flow through topaz to satisfy the continuity equation, and this seeks to reduce the temperature. On the other hand, by increasing the porosity, the equivalent conductivity in the porous zone decreases (see Eq.7), and as the heat transfer rate from the plates to the topaz water mixture depends to a great extent on the equivalent conductivity of the adjacent layer of the mixture in the radial direction, this effect seeks to cause an increase in the plate temperature and hence the topaz-water layer adjacent to the plates which seeks to increase the average topaz temperature. Initially, at small values of porosity, with an increase in porosity, the effect of increasing the velocity of fluid flow on the temperature is greater than the effect of the decrease in the thermal conductivity, so the resultant is a decrease in the average temperature. This trend of average temperature with porosity continues until a certain value of porosity (about 0.2), after which the increase of porosity causes the effect of conductivity to be superior to the effect of water velocity, such that the average temperature starts to increase. So, the value of porosity at which minimum average temperature obtained, which is 0.2 as indicated in Fig.11, is considered to be the ideal theoretical value of porosity for best thermal characteristics. This value is considered the ideal value theoretically as it may be unpractical to obtain a value of porosity lower than 0.3. So, practically, it can be said that the ideal value of porosity from the thermal-hydraulic point of view is the lowest porosity which can be practically obtained although the porosity without considering the variation of heat generation in topaz has a slight effect on the average temperature values as shown from in Fig.11.

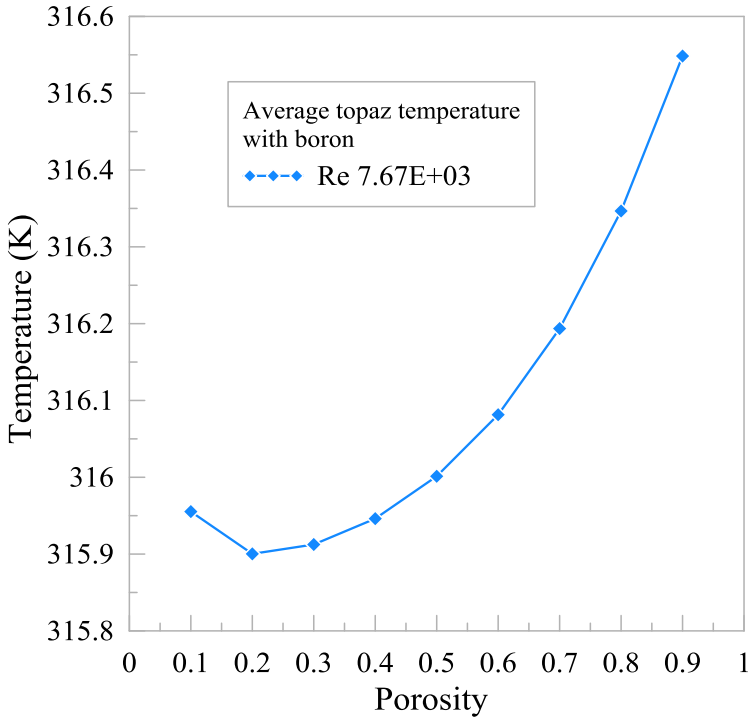

Fig.11 Variation of average topaz temperature with porosity for the case of irradiation with the plates

4.4 Development of average Nu correlations

The definition of Nu is Nu = hD/k, where D is the hydraulic diameter of the irradiation box and k is the conductivity of the coolant. So, Nu has the same trend as the trend of the heat transfer coefficient discussed in section 4.2.The values of Nu over the Boron carbide plate were validated in section 3 (see Fig.3). Data fit of these values can correlate them with Re and ε, in their studied range, to give the following correlation:

$$Nu = 0.0502305 Re^{0.66290} (Pr/\varepsilon)^{0.25679} \qquad (12)$$

Similarly, a correlation can be obtained for average Nu over topaz relating it with both Re and ε. This correlation is:

$$Nu = 5.11441\text{E} - 05 Re^{1.08124} (Pr/\varepsilon)^{0.7157} \qquad (13)$$

V. CONCLUSION

Three dimensional CFD thermal-hydraulic analysis is carried out for the irradiation process of topaz in ETRR-2. Flow and heat transfer characteristics are determined for both the cases of the modified irradiation process in which there are Boron-Carbide plates at the sides of the topaz irradiation box and the irradiation process without the plates. The following conclusions can be stated:

1- The maximum temperature throughout the topaz box is at the box corner, at the exit from the box for all the cases.

2- For the case of irradiation with Boron-Carbide plates, the maximum temperature value increases with the porosity and decreases with Re. Onset of nucleate boiling can occur at the exit corner of the box for porosity greater than 0.4 at a value of $Re = 2.23x10^2$, for the studied range of Re and porosity.

3- Onset of nucleate boiling can be prevented either by working at a flow rate of inlet velocity greater than 1.4 m/s or porosity lower than 0.4.

4- The average topaz temperatures for the case of irradiation without the Boron- carbide plates are greater than the corresponding ones for irradiation with the plates.

5- By decreasing the porosity, the average topaz temperature decreases and the heat transfer coefficient increases for the case of irradiation with the Boron-Carbide plates and the reverse occurs for irradiation without the plates.

6- The average topaz temperature decreases with Re for both the cases of irradiation with or without the Boron-Carbide plates.

7- For the case of irradiation with the Boron-Carbide plates, the ideal value of porosity from the thermal hydraulic point of view is theoretically 0.2 and practically the lowest porosity that can be obtained as a porosity of 0.2 cannot be obtained practically.

8- Data fit of the present results of Nu can correlate it with Re and ε in their studied range to give two best fit correlations which are Eq.12 and 13 for Nu over the Boron-Carbide plate and topaz respectively.

REFERENCES

[1]. Ashbuugh, Charles E., Gemstone Irradiation and Radioactivity, Gemological Institute of America 1989.
[2]. Nassau, Kurt, Altering the colour of topaz. Gems & Gemology, Gemological Institute of America, 1985. .
[3]. Nassau, Kurt, The Causes of Colour. Scientific American, Inc, 1980.
[4]. Raju, K.S., Topaz-on neutron irradiation. Int. J. Appl. Radiat. Isot. 32, 1981.
[5]. Noomie Lewinson, Electron beam enhancement of colourless topaz, www.cigem.ca/pdf/noomie.pdf, 2015.
[6]. Nassau, Kunr, Prescott, Brrry E., Blue and brown topaz produced by gamma irradiation. Am. Mineral. 60, 1975.
[7]. Nader M.A. Mohamed , M.A. Gaheen, Design of fast neutron channels for topaz irradiation, Nuclear Engineering and Design, 2016.
[8]. A Maneewong, K Pangza, T Charoennam, N Thamrongsiripak and N Jangsawang, The Impact of Electron Beam Irradiation in topaz Quality Enhancement, IOP Conf. Series: Journal of Physics: Conf. Series1285, 2019.
[9]. International Atomic Energy Authority (IAEA), The Applications of Research Reactors IAEA-TECDOC-1234. IAEA, 2001.
[10]. Ranz W. E. & Marshall W. R. "Evaporation from drops", Chem. Eng.18 Proc. 48, 173–180 (1952).
[11]. Whitaker S. "Forced convection heat transfer correlations for flow in pipes, past flat plates, single cylinders, single spheres, and flow in packed beds and tube bundles", AIChE J 18, 361–371 (1972).
[12]. Macias-Machin, A., Oufer, L., Wannenmacher, N., 1991, "Heat transfer between an Immersed Wire and a Liquid Fluidized Bed" Powder Technology, vol. 66:281-284, 1991.
[13]. Gnielinksi, V., "Calculation of the heat and mass transfer flows through the beds
[14]. ", Verfahrenstechnik 16, 36, 1982.
[15]. P.Cheng, " Combined forced and free convection flow about inclined surfaces in porous media", Int. J of Heat and Mass Transfer 20, 807 814,1977.
[16]. Spechia, V. Baldi, G., Sicardi, S., "Heat transfer in packed bed reactors with one phase flow", Chem. Eng. Comm. 4, 361, 1980.
[17]. Kunii, F., Smith, J.M., "Heat Transfer Characteristics of Porous Rocks", AIChE J. 6, 71, 1960.
[18]. Y. Demirel*, R.N. Sharma, H.H. Al-Ali, "On the effective heat transfer parameters in a packed bed", International Journal of Heat and Mass Transfer 43 327-332, 2000.
[19]. S. El-Din El-Morshdy, S., Thermal-hydraulic assessment of topaz irradiation processes at the ETRR-2 research reactor, kerntechnik, 2005.
[20]. Fluent, A. (2020). ANSYS fluent theory guide V. 20.0. Ansys: inc.